Prompt ν_τ fluxes in present and future τ neutrino experiments

M. C. Gonzalez-Garcia*
Theory Division, CERN, CH-1211 Geneva 23, Switzerland

J. J. Gomez-Cadenas†
PPE Division, NOMAD experiment, CERN, CH-1211 Geneva 23, Switzerland
(Received 13 August 1996)

We use a nonperturbative QCD approach, the quark-gluon string model, to compute the τ-neutrino fluxes produced by fixed target pA collisions (where A is a target material) for incident protons of energies ranging from 120 to 800 GeV. The purpose of this calculation is to estimate *in a consistent way* the prompt background for the $\nu_\mu(\nu_e)\leftrightarrow\nu_\tau$ oscillation search in the on-going $\nu_\mu(\nu_e)\leftrightarrow\nu_\tau$ oscillation search experiments CHORUS and NOMAD, as well as the expected prompt background in future experiments, such as COSMOS at Fermilab and a possible second-generation $\nu_\mu(\nu_e)\leftrightarrow\nu_\tau$ search experiment at the CERN SPS. In addition, we compute the number of ν_τ interactions expected by the experiment E872 at Fermilab. [S0556-2821(97)04703-6]

PACS number(s): 14.60.Lm, 11.15.Tk, 14.60.Pq

I. INTRODUCTION

In proton-proton and proton-nucleus collisions, the main source of τ neutrinos is the leptonic decay of the secondary D_s meson, $D_s\rightarrow\tau\nu_\tau$. The possibility of producing a τ neutrino beam from this source has been investigated by several authors (see [1,2] and references therein). At present, there is an approved experiment, E872 [2], which aims at detecting about 200 ν_τ charged current interactions in an emulsion target intercepting a ν_τ beam originated by the decays of the D_s mesons produced when the Fermilab 800 GeV proton beam hits a tungsten target.

On the other hand, the ongoing $\nu_\mu(\nu_e)\leftrightarrow\nu_\tau$ oscillation search experiments CHORUS and NOMAD [3,4], are taking data in the CERN Super Proton Synchrotron (SPS) wide band neutrino beam. This beam consists primarily of ν_μ's with a small contamination of $\overline{\nu_\mu}$, ν_e, and $\overline{\nu_e}$. The experiments aim at reaching a sensitivity to $\nu_\mu(\nu_e)\leftrightarrow\nu_\tau$ oscillations in the range $P(\nu_\mu\rightarrow\nu_\tau)<2-4\times10^{-4}$. In order to do so, backgrounds have to be controlled typically down to the 10^{-6} level. Both experiments are confident that the τ signature in their apparatus is distinctive enough to reduce the huge contamination due to $\nu_\mu(\nu_e)$ charged and neutral currents to a very small level. On the other hand, the contamination of ν_τ's in the ν_μ beam represents an irreducible background which was, however, estimated to be negligible ($R_\tau=\nu_\tau CC/\nu_\mu CC\sim10^{-7}$) at the time of the NOMAD and CHORUS proposals [3,4]. However, a recent new estimation [5] yields a surprisingly high result, $R_\tau\sim3.3\times10^{-6}$, a factor of 30 higher than previous estimations.

In [5], several possible sources of prompt ν_τ's are evaluated. As naively expected, the only relevant source of ν_τ's is the leptonic decay $D_s\rightarrow\tau\nu_\tau$, followed by $\tau\rightarrow\nu_\tau+X$. To estimate this background, the kinematic quantities of charm hadroproduction are parametrized in the conventional way,

$$\frac{d^2\sigma}{dx_F dp_T^2}\sim(1-|x_F|)^n e^{-bp_T^2}, \tag{1}$$

and an ''educated guess'' of the value of the n parameter, $n=5.5$, is used. Indeed, the same approach is used in the proposal of the COSMOS experiment [6] [a proposed $\nu_\mu(\nu_e)\leftrightarrow\nu_\tau$ oscillation search at Fermilab which aims to reach a sensitivity a factor 10 higher than CHORUS and NOMAD] and in the E872 [2] proposal. Unfortunately, this implies using different ''educated guesses'' in every case. Furthermore, present experimental data allow for large variations in the value of n for charm production at different energies, which in turn results in large uncertainties concerning the final result.

Alternatively to use an empirical parametrization, we evaluate the prompt ν_τ background by using a theoretically well-understood framework. Specifically, we use the quark-gluon string model (QGSM), which provides (a) a prediction of the hadroproduction cross section of charmed mesons, which agrees well with available data, (b) a prediction of the fraction of D_s mesons relative to the total charm cross section, and (c) a prediction of $d^2\sigma/dx_F dp_T^2$.

Perturbative QCD, which gives a good description for hard processes at the parton level, fails to describe the spectra of produced hadrons. To describe the processes of multihadron production at high and medium energies, wide use has been made of models based on the idea of the $1/N$ expansion of QCD [7,8]. A well-known nonperturbative QCD approach to the description of hadron processes is the quark gluon string model [9–16]. The QGSM has proven to describe with great success the production of hadrons containing light quarks. It also describes adequately the production of charmed mesons, and thus it can be applied in a straightforward way to compute neutrino fluxes due to the tauonic decay of the D_s meson [1]. Although the QGSM is not, strictly speaking, a ''theory'' directly derived from first prin-

*Electronic address: concha@vxcern.cern.ch
†On leave from Department of Physics and Astronomy, University of Massachusetts, Amherst, and Departamento de Física Atómica y Nuclear, Universidad de Valencia, Spain. Electronic address: gomez@axnd02.cern.ch

ciples but rather a model based on quark-parton ideas, QCD string dynamics and Reggeon calculus, it has two appealing features. First, it has achieved great success in describing existing data on particle hadroproduction, including charm. Second, it is based on simple and well-understood principles.

This paper is organized as follows. The QGSM is briefly sumarized in Sec. II. In Sec. III we compute cross sections and longitudinal momentum distributions for charmed mesons and show that the QGSM describes well existing charm data. Section IV contains the relevant formulas to compute ν_τ fluxes. In Sec. V we use the QGSM to obtain a prediction for the ν_τ contamination in the CHORUS experiment. We also show that the error introduced in the calculation by the ''tunable'' parameters of the model (see Sec. II) is negligible. The background expected by the NOMAD experiment is computed in Sec. VI. In Sec. VII we obtain the number of ν_τ interactions expected by three future experiments. COSMOS, E872, and a possible next generation $\nu_\mu(\nu_e)\leftrightarrow\nu_\tau$ oscillation experiment at CERN-SPS. Finally we summarize our results in Sec. VIII.

II. THE QUARK GLUON STRING MODEL

The QGSM is a nonperturbative model which describes soft hadronic processes. The model is based on the theory of the supercritical Pomeron and on the $1/N$ expansion of the amplitudes in QCD where N can correspond to the number of colors [7] or flavors [8]. At high energies, the $1/N$ expansion of QCD is equivalent to the topological expansion which implies that interactions represented by topologically complicated diagrams are suppressed by powers of N^{-1}. The QGSM is similar to the dual parton model [17] but they differ in the fragmentation functions. The model can be used to quantitatively describe in terms of few parameters the main characteristics of multiple production of hadrons in hadron-hadron and hadron-nucleus interactions, such as particle multiplicity for different flavors, rapidity distributions of the produced hadrons, the KNO scaling and the deviations as well as the behavior of the total and elastic cross sections.

In the approach of the QGSM the production of hadrons is described in terms of Pomeron exchange (cylindrical graphs) and Reggeon exchange (planar graphs). In the planar case the annihilation of the valence quarks of the colliding hadrons leads to a configuration of a single-color tube whose breaking gives rise to the appearance of white (colorless) hadrons. Planar diagrams behave as $1/\sqrt{s}$ at large s and in consequence they die off at large energies. The simplest and dominant contribution which does not vanish at large energies is the single Pomeron exchange in which the colliding hadrons exchange one or several gluons (as opposed to valence quarks in the planar graphs). The corresponding diagram has the topology of a cylinder. A unitary cut gives two chains of hadrons which have properties similar to those of the planar case. In addition, in the QGSM the possibility of exchange of several Pomerons is also accounted for in accordance with Reggeon calculus. Multi-Pomeron diagrams correspond to the successive terms of the $1/N$ expansion.

Once the dominant diagrams have been classified, the model gives a well-defined prescription for associating a cross section with each diagram in the expansion. These diagrams have a direct correspondence with the ones used in Reggeon field theory and this is used to obtain the weights of each diagram. In order to do so, the Abramovskii-Gribov-Kancheli cut rules are used. They permit the calculation of the cross section for the n-pomeron cut in the quasieikonal approximation as [9]

$$\sigma_n^{pp}(\xi)=\frac{\sigma_P}{nz}\left(1-\exp(-z)\sum_{k=0}^{n-1}\frac{z^k}{k!}\right),$$

where

$$z=\frac{2C\gamma_P}{R^2+\alpha'_P\xi}\exp(\xi\Delta), \tag{2}$$

and $\sigma_P=8\pi\gamma_P\exp(\xi\Delta)$, $\xi=\ln(s/1\text{GeV}^2)$. The total cross section is the sum of the cross sections σ_n,

$$\sigma_{\text{tot}}^{pp}(\xi)=\sum_{n=0}^{\infty}\sigma_n^{pp}\xi=\sigma_P f\left(\frac{z}{2}\right),$$

$$f(z)=\sum_{\nu=1}^{\infty}\frac{(-z)^{\nu-1}}{\nu\nu!}=\frac{1}{z}\int_0^z\frac{dx}{x}[1-\exp(-x)], \tag{3}$$

while the inelastic cross section is given by

$$\sigma_{\text{in}}^{pp}(\xi)=\sigma_{\text{DD}}+\sum_{n=1}^{\infty}\sigma_n(\xi). \tag{4}$$

σ_{DD}^{pp} is the cross section of diffractive dissociation of one of the initial protons

$$\sigma_{\text{DD}}=\frac{C-1}{C}\sigma_P[f(z/2)-f(z)]. \tag{5}$$

The parameters γ_P and R^2 characterize the hadron-Pomeron vertex and C gives the relative contribution of the diffractive dissociation. These parameters are obtained by fitting existing data on elastic pp and $p\bar{p}$ scattering and diffractive processes. We use $\gamma_P=3.64$ GeV^{-2}, $R^2=3.56$ GeV^{-2}, $C=1.5$, $\alpha'_P=0.25$ GeV^{-2}, and $\Delta=0.07$ [9] which are valid for the not very high energies we are working at. For higher enegies the best values are $\gamma_P=1.77$ GeV^{-2}, $R^2=3.18$ GeV^{-2}, $C=1.5$, $\alpha'_P=0.25$ GeV^{-2}, and $\Delta=0.139$ [11].

Once the weight of the different diagrams is determined, to compute inclusive cross sections for the production of secondary hadrons it is also necessary to know the distribution functions of the quarks and diquarks in the colliding hadrons and the fragmentation functions of quarks and diquarks into secondary hadrons. In the QGSM it is assumed that all these functions are determined in the regions $x\to1$ and $x\to0$ by the corresponding Regge asymptotic behaviors and in the intermediate region by means of interpolation. This method allows the imposition of several conservation laws that must be verified, for example, momentum conservation which implies that the sum of momenta of all the constituents in a hadron must be equal to the momentum of the hadron. In the fragmentation process the momentum must also be conserved as well as electric charge, baryon, and flavor quantum numbers, etc.

With all this in mind the inclusive cross section for the production of a hadron h in p-p collisions can be written as [9,10]

$$\frac{1}{\sigma_{\rm in}}\frac{d\sigma^h}{dy}=\sum_{n=1}^{\infty} w_n(s)\phi_n^h(s,y)+V_D^{(1)}\phi_D^{h(1)}(s,y)+V_D^{(2)}\phi_D^{h(2)}(s,y), \tag{6}$$

where $w_n=\sigma_n/\sigma_{\rm in}$ is the probability of cutting n Pomerons. $y=1/2\ln[(E+p_\parallel)/(E-p_\parallel)]$ is the rapidity of the secondary hadron in the center of mass frame and $\phi_n^h(s,y)$ are the y distributions of the hadron h in the $2n$-chain process:

$$\phi_n^h=a^h[F_q^{h(n)}(x_+)F_{qq}^{h(n)}(x_-)+F_q^{h(n)}(x_-)F_{qq}^{h(n)}(x_+)+2(n-1)F_{q\rm sea}^{h(n)}(x_+)F_{q\rm sea}^{h(n)}(x_-)], \tag{7}$$

where

$$x_\pm=\frac{1}{2}(\sqrt{x_\perp^2+x^2}\pm x),\quad x=\frac{2p_\parallel}{\sqrt{s}},\quad x_\perp=\frac{2\sqrt{m_h^2+p_\perp^2}}{\sqrt{s}}. \tag{8}$$

The piece in $V_D^{(1)}$ represents the contribution from the diffractive dissociation of the incident hadron and it is given by

$$V_D^{(1)}=\frac{\sqrt{C}}{\sqrt{C}+1}\frac{\sigma_{\rm DD}}{\sigma_{\rm in}},$$

$$\phi_D^{h(1)}=3a^h[\sqrt{x_+}F_{1qq}^{h(1)}(x_+)+\sqrt{x_-}F_{1qq}^{h(1)}(x_-)]$$

for h being a nucleon or Λ baryon,

$$\phi_D^{(1)}=3a^h[\sqrt{x_+}+\sqrt{x_-}]F_q^{h(1)}(x_+)F_q^{h(1)}(x_-)$$

for other hadrons. (9)

Finally the last term in Eq. (6) gives the contribution due to diffractive dissociation of the target and it is described by the sum of the triple Reggeon diagrams. For secondary protons one has

$$\phi_{PPP}^{p(2)}=\frac{0.065}{(1-|x|)B}\exp\left(-B\frac{(1-|x|)^2}{|x|}m_p^2\right),$$

$$B=[4-0.6\ln(1-|x|)]{\rm GeV}^{-1},$$

$$\phi_{PPR}^{p(2)}=\frac{3.3}{\sqrt{s(1-|x|)}}\phi_{PPP},$$

$$\phi_{RRR}^{p(2)}=0.1x^2\sqrt{350\ {\rm GeV}^2/{\rm s}}, \tag{10}$$

and $V_D^{(2)}=1$. B gives the slope of the diffractive peak. For secondary neutrons $V_D^{(2)}=2/3$ and only the RRR diagram contributes.

The functions F in Eq. (7) are given by

$$F_q^{h(n)}(x)=\frac{2}{3a_h}\int_x^1 dx_1 f_p^{u(n)}(x_1)G_u^h\left(\frac{x}{x_1}\right)+\frac{1}{3a_h}\int_x^1 dx_1 f_p^{d(n)}(x_1)G_d^h\left(\frac{x}{x_1}\right),$$

$$F_{qq}^{h(n)}(x)=\frac{2}{3a_h}\int_x^1 dx_1 f_p^{ud(n)}(x_1)G_{ud}^h\left(\frac{x}{x_1}\right),$$

$$F_{q\rm sea}^{h(n)}(x)=\frac{1}{(4+2\delta)a_h}\int_x^1\left\{dx_1 f_p^{u{\rm sea}(n)}(x_1)\times\left[G_u^h\left(\frac{x}{x_1}\right)+G_{\bar u}^h\left(\frac{x}{x_1}\right)\right]+f_p^{d{\rm sea}(n)}(x_1)\left[G_d^h\left(\frac{x}{x_1}\right)+G_{\bar d}^h\left(\frac{x}{x_1}\right)\right]+\delta f_p^{s{\rm sea}(n)}(x_1)\left[G_s^h\left(\frac{x}{x_1}\right)+G_{\bar s}^h\left(\frac{x}{x_1}\right)\right]\right\}. \tag{11}$$

$f^{i(n)}(x)$ are the distribution of quarks and diquarks with fraction of energy x in the proton. $G_i^h(z)$ are the fragmentation functions of the quark or diquark chain into a hadron h which carries a fraction z of its energy. The distribution functions can be written in terms of the intercepts $\alpha_R=0.5$, $\alpha_N=-0.5$, and $\alpha_\phi=0$ of known Regge poles. The parameter δ takes into account the possibility of appearance of chains whose ends are connected to strange quarks from the sea and it is taken to be $\delta=0.3$.

The behavior of the fragmentation functions in the asymptotic limits is also determined by Regge theory. In the limit $x\to 0$, $G_i^h(x)\to a_h$, where a_h is a constant determined by the dynamics of the rupture of the string [10]. It cannot be calculated directly but it is fitted from data taking into account that all particles in the same isotopic multiplet have the same constant a^h.

In the limit $x\to 1$, the behavior of the fragmentation function is determined by the intercept of the corresponding Regge trajectory and it depends on whether the hadron contains the fragmented quark or diquark (favored fragmentation) or it does not contain it (forbidden fragmentation) [10]. A full list of the different fragmentation functions can be found in Refs. [11–13,16]. A remark must be done when the produced hadron is a baryon. In this case Eq. (7) is modified to be [16]

$$\phi_n^h=a^h[F_{1qq}^{h(n)}(x_-)+F_q^{h(n)}(x_+)F_{2qq}^{h(n)}(x_-)+F_{1qq}^{h(n)}(x_+)+F_q^{h(n)}(x_-)F_{2qq}^{h(n)}(x_+)+2(n-1)F_{q\rm sea}^{h(n)}(x_+)F_{q\rm sea}^{h(n)}(x_-)], \tag{12}$$

where F_{2qq} presents the same asymptotic behavior discussed above while the piece in F_{1qq} represents the ''string junction'' of the diquark.

The QGSM fragmentation functions into charmed mesons is determined as $z\to 1$ by α_ψ, the intercept of the $c\bar c$ Regge trajectory, on which we have no direct empirical information. If one assumes that, as in the case of light quarks, the $c\bar c$ trajectories are linear and exchange-degenerate, then, from the masses of the 2^+ $\chi(3555)$ and 1^- $\psi(3100)$ states,

the slope of the ψ trajectory is $\alpha_\psi \sim -2.2$ GeV^{-2}. On the other hand, it may be supposed that the parameters of the ψ trajectory are dictated by perturbation theory on QCD. In this case $\alpha_\psi \sim 0$ GeV^{-2} and the trajectory should be strongly nonlinear [12]. We will consider the linear and perturbative values as the two extremes of the model predictions.

Equation (6) is valid for pp collisions. For p-nucleus interactions the structure of the interaction remains basically the same. However one has to take into account the possibility of interactions with more than one nucleon. Following the approach in Ref. [14] we describe the cross section for inelastic interactions of the incident proton with ν nucleons in the two-channel model:

$$\sigma_{hA}^{\nu}=\frac{1+\cos\theta}{2}\int d^2b\frac{1}{\nu!}[\lambda_1\sigma_1^{\rm in}T(b)]^{\nu}\exp[-\lambda_1\sigma_1^{\rm in}T(b)] + \frac{1-\cos\theta}{2}\int d^2b\frac{1}{\nu!}[\lambda_2\sigma_2^{\rm in}T(b)]^{\nu}\exp[-\lambda_2\sigma_2^{\rm in}T(b)], \tag{13}$$

where

$$\sigma_{1,2}^{\rm in}=\sigma_{pp}^{\rm tot}-\lambda_{1,2}\sigma_{pp}^{\rm el}, \quad \lambda_{1,2}=\frac{1+d\pm X}{2}, \qquad X^2=(1-d)^2+4g^2, \quad \cos\theta=\frac{1-d}{X}, \tag{14}$$

$g^2\simeq 0.2$ gives the probability of diffractive excitation of the incident hadron and $d\simeq 1$ gives the probability of beam-beam interaction relative to the hadron-hadron one.

Hadrons are also produced in diffractive dissociation of the incident hadron with a cross section

$$\sigma_{pA}^{\rm diff}=\frac{\sin^2\theta}{4}\int d^2b[\exp[-\lambda_1\sigma_1^{\rm in}T(b)]+\exp[-\lambda_2\sigma_2^{\rm in}T(b)] -2\exp[-(\lambda_1+\lambda_2)\sigma_{12}^{\rm in}T(b)/2], \tag{15}$$

where $\sigma_{12}^{\rm in}=\sigma_{pp}^{\rm tot}-2\lambda_1\lambda_2/(\lambda_1+\lambda_2)\sigma_{pp}^{\rm el}$. In all the expressions above, $T(b)$ is the matter density distribution in the impact parameter space $T(b)=A\int_{-\infty}^{\infty}\rho(b,z)dz$. For light nuclei such as beryllium, we use the density given by the shell model:

$$T(b)=\frac{1}{3\pi r_0^4}\exp(-b^2/r_0^2)[(8+A)r_0^2-(8-2A)b^2]. \tag{16}$$

r_0 is a parameter which is determined from the experimental measured value of the mean radius of the nucleus. For ^{9}Be, $r_0=1.74$ fm for the shell model.

For heavy nuclei we use the Woods-Saxon density

$$T(b^2)=A\int dz\rho(r=\sqrt{z^2+b^2}), \qquad \rho(r)=\rho_0\frac{1}{1+\exp[(r-c_1)/c_2]} \quad \text{with} \quad \int 4\pi r^2dr\rho(r)=1, \tag{17}$$

with $c_1=1.15A^{1/3}$ fm and $c_2=0.51$ fm.

Thus the total cross section for production of at least one secondary particle is given by

$$\sigma_{\rm in}(pA)=\sigma_{pA}^{\rm diff}+\sum_{\nu=1}^{A}\sigma_{pA}^{\nu}. \tag{18}$$

III. CHARM AND THE QGSM

The QGSM has proven to be very successful in describing the experimental data on secondary hadron production in both proton-proton and proton-nucleus collisions in the intermediate energy region. It also describes quite well the scarce experimental data on charm production [1,12,13,18–21]. Clean and reliable data on charmed meson production in pp collisions have been obtained by the LEBC-EHS and LEBC-MPC Collaborations at $\sqrt{s}=24.3$ GeV, $\sqrt{s}=27.4$ GeV, and $\sqrt{s}=38.8$ GeV [18]. Recently the E769 Collaboration has published results on inclusive charm distributions on pN collisions at $\sqrt{s}=21.6$ GeV. The only data on charm production at high energy was obtained in the CERN $p\bar{p}$ collider at $\sqrt{s}=630$ GeV [19] by measuring the production of prompt electrons of relatively low $p_\perp$. The recent measurement of the inclusive charm cross section by the HELIOS Collaboration [21] also relies on the measurement of low $p_\perp$ prompt electrons as well as muons.

The QGSM has not been developed to the point of predicting the transverse momentum spectrum of the produced hadrons. To describe the transverse momentum distribution of particles of mass m in the forward cone of interest to neutrino physics we use the same approach as in [1] and adopt the classical thermodynamical model of Koppe and Fermi [22] as elaborated by Hagedorn [23] and collaborators. In this model the transverse momentum distributions are essentially exponential in m_T/T where $m_T=\sqrt{m^2+p_\perp^2}$ is the transverse mass and T is and effective ''temperature'' which is a function of the center of mass energy:

$$\frac{d\sigma}{dp_\perp}=Tp_\perp\sqrt{m_T}\exp\left(-\frac{m_T}{T}\right). \tag{19}$$

In [1] the existing data were fitted to this expression with a T function of the form $T=a+b[\ln(s/\text{GeV}^2)]^c$. We use their result

$$a=0.128\pm 0.002 \text{ GeV}, \qquad b=(1.5\pm 1.4)\times 10^{-8} \text{ GeV}, \qquad c=5.9\pm 0.8. \tag{20}$$

With all these elements we have written a particle generator which we use to predict the charmed hadron distributions produced in pp as well as pA (with A being a nucleus) collisions. To illustrate how the QGSM describes the existing data on charmed meson production, in Fig. 1 we show the differential cross sections for the different D mesons measured by LEBC-EHS [18] (notice that the experiment took data at $\sqrt{s}=27.4$ GeV, very close to the center of mass energy of the 450 GeV protons of the SPS colliding against a fixed target) and compare them with the QGSM predictions

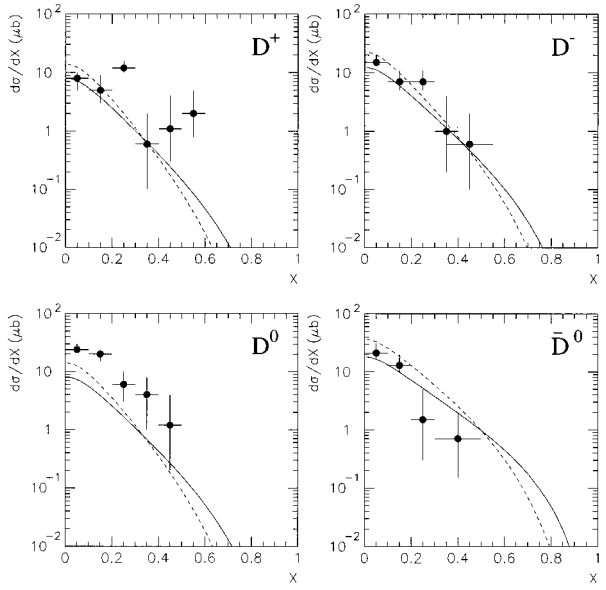

FIG. 1. Predictions of the QGSM for the Feynman-x distribution of charmed mesons at 27.4 GeV for $\alpha_\psi=0$ (solid line) and $\alpha_\psi=-2.2$ (dashed line) compared with the data.

for $\alpha_\psi=0$ and $\alpha_\psi=-2.2$. The agreement is quite satisfactory except in the case of the D^0 distributions, which are harder in the data than predicted by the model. As discussed in [12,1], this result can be due to bad particle identification. Notice that in pp interactions, at (relatively) low energies one would expect to observe a spectrum of $D^0(u\bar{c})$ harder than that of $D^0(\bar{u}c)$, since the former meson can be produced directly on the leading u quarks of the colliding protons.

In Fig. 2 we show the inclusive spectra of D mesons

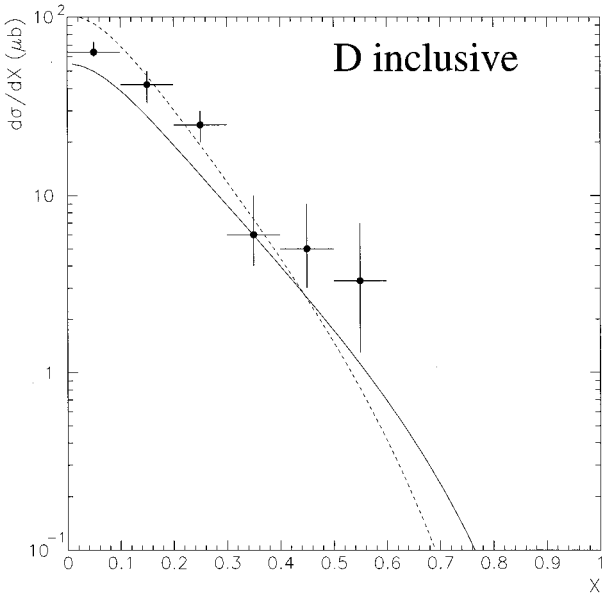

FIG. 2. Predictions of the QGSM for the Feynman-x distributions of inclusive charmed meson cross section at 27.4 GeV for $\alpha_\psi=0$ (solid line) and $\alpha_\psi=-2.2$ (dashed line) compared with the data.

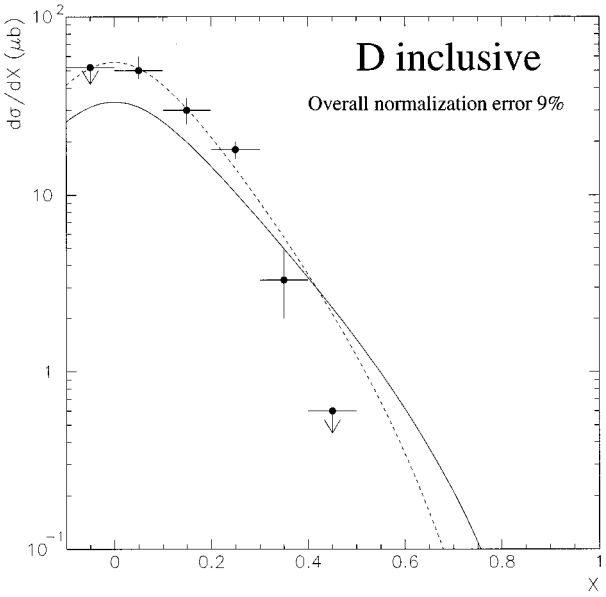

FIG. 3. Predictions of the QGSM for the Feynman-x distributions of inclusive charmed meson cross section at 22.6 GeV for $\alpha_\psi=0$ (solid line) and $\alpha_\psi=-2.2$ (dashed line) compared with the data.

measured by LEBC-EHS [18] together with the model predictions while in Fig. 3 we show the inclusive spectra of D mesons measured by the E769 experiment. Notice that while the LEBC-EHS data are fairly well described with both values of α_ψ, the E769 data are better described by the model with $\alpha_\psi=-2.2$. Finally, in Fig. 4 we show the existing data on the total charm cross section together with the model predictions.

To summarize, we believe that the QGSM is the most satisfactory of the tools available to describe charm produc-

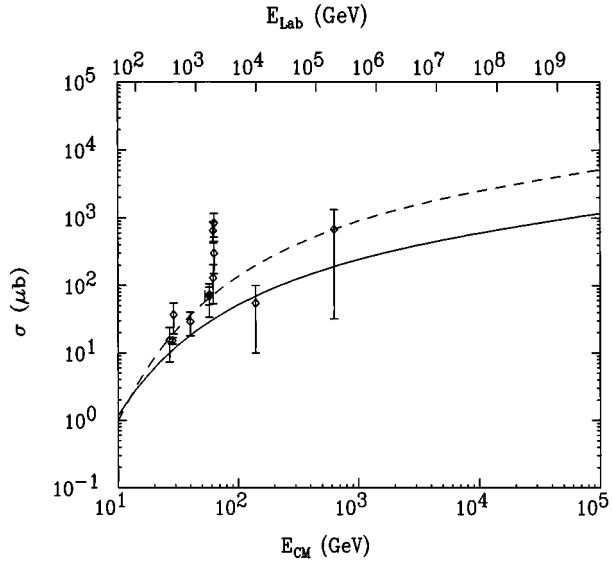

FIG. 4. Predictions of the QGSM for the total charm cross section as a function of the energy for $\alpha_\psi=0$ (lower solid line) and $\alpha_\psi=-2.2$ (lower dashed line) assuming $\sigma_{c\bar{c}}=1/2\sigma_{D/\bar{D}}$ and a selection of experimental points.

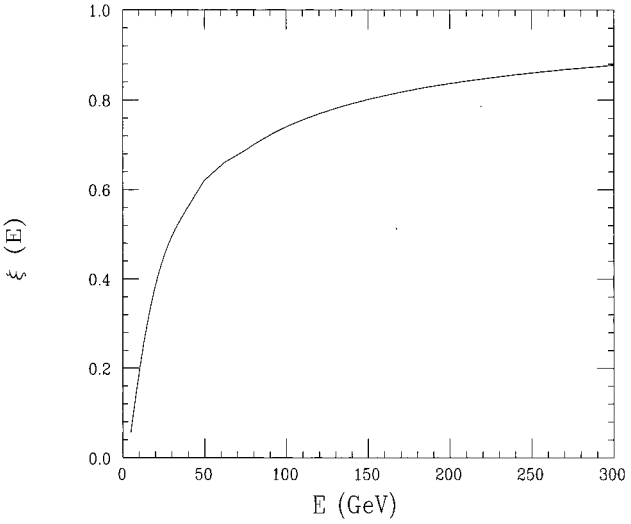

FIG. 5. Ratio of the $\nu_\tau N \to \tau X$ to $\nu_\mu N \to \mu X$ cross section as a function of the neutrino energy.

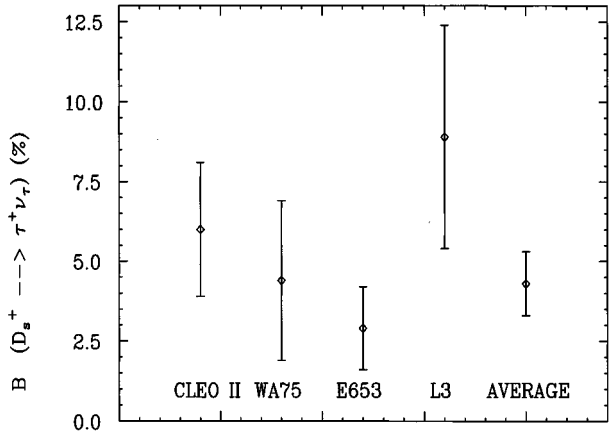

FIG. 6. Recent measurements of the branching ratio $B(D_s \to \tau \nu_\tau)$.

tion at modest momentum transfer. It describes well an impressive number of features of hadronic interactions and all the recent data on charm production at available energies.

IV. FORMULAS FOR ν_τ FLUX CALCULATION

In pA collisions (where A is a nuclear target), τ neutrinos are produced either directly in the decay of $D_s^+ \to \tau^+ \nu_\tau$ or through the chain $D_s^- \to \tau^- \overline{\nu}_\tau (\tau^- \to \nu_\tau + X)$. We will denote $\nu_{\tau 1}$ the neutrino produced in the direct D_s^+ decay and $\nu_{\tau 2}$ the one produced in the subsequent τ^- decay. The number of neutrinos produced in each of these processes is

$$N_{\nu_\tau i} = \frac{\sigma(pA \to D_s^+)}{\sigma_{\rm in}(pA)} \times B(D_s^+ \to \tau^+ \nu_\tau) \times \mathrm{POT} \times \alpha, \quad (21)$$

where the number of protons in target (POT) is defined as the total number of protons delivered by the beam to the target, and α is the fraction of protons that interact in the target.

The interaction cross section for ν_τ's can be written as

$$\sigma_{\nu_\tau N} = \sigma_\nu^0 \times \xi_{\rm thres}(E_{\nu_\tau}) \times E_{\nu_\tau} = 6.7 \times 10^{-3} \times \xi_{\rm thres}(E_{\nu_\tau}) \times \frac{E_{\nu_\tau}}{\mathrm{GeV}} \frac{\mathrm{pb}}{\mathrm{nucleon}}, \quad (22)$$

where $\sigma_\nu^0 = 6.7 \times 10^{-3}$ pb/GeV and the factor $\xi_{\rm thres} = \sigma_{\nu_\tau CC}/\sigma_{\nu_\mu CC}$ (see Fig. 5) takes into account the deviation of the linearity in the interaction cross section due to the τ mass. The number of ν_τ interactions in the target originated by the neutrino produced in the D_s^+ decay is then

$$N_{\nu_\tau} CC1 = N_{\nu_\tau 1} \times \sigma_{\nu_\tau 1} \times \mathrm{Acc}_{\nu_\tau 1} \times N_A \times \rho \times d(\theta), \quad (23)$$

where $\sigma_{\nu_\tau 1}$ is the interaction cross section, $\mathrm{Acc}_{\nu_\tau 1}$ the geometrical acceptance (defined as the fraction of ν_τ's which hit the target), N_A the Avogadro number, ρ the target density, and $d(\theta)$ is the distance crossed by the neutrinos in the target, which is a function of the incoming angle. If L is the target length, we can rewrite Eq. (23) as

$$N_{\nu_\tau} CC1 = N_{\nu_\tau 1} \times \sigma_{\nu_\tau 1} \times \mathrm{Acc}_{\nu_\tau 1} \times N_A \times \rho \times L \times r(\theta) \quad (24)$$

with $r(\theta) = d(\theta)/L$. Thus we obtain

$$\frac{N_{\nu_\tau} CC1}{N_{\nu_\mu} CC} = R_0 \times \langle E_{\nu_\tau 1} \times \xi_{\nu_\tau 1} \times r \rangle \times \mathrm{Acc}_{\nu_\tau 1} \times \frac{\sigma(pA \to D_s^+)}{\sigma_{\rm in}(pA)} \times B(D_s^+ \to \tau^+ \nu_\tau) \frac{\mathrm{POT}}{N_{\nu_\mu} CC} \times \alpha, \quad (25)$$

where $R_0 = \sigma_0 \times N_A \times \rho \times L$. Analogously, we will have, for the neutrino produced through the chain $D_s^- \to \tau^- \overline{\nu}_\tau (\tau^- \to \nu_\tau + X)$,

$$\frac{N_{\nu_\tau} CC2}{N_{\nu_\mu} CC} = R_0 \times \langle E_{\nu_\tau 2} \times \xi_{\nu_\tau 2} \times r \rangle \times \mathrm{Acc}_{\nu_\tau 2} \times \frac{\sigma(pA \to D_s^+)}{\sigma_{\rm in}(pA)} \times B(D_s^+ \to \tau^+ \nu_\tau) \times \frac{\mathrm{POT}}{N_{\nu_\mu} CC} \times \alpha. \quad (26)$$

The value of the constant R_0 and the ratio $N_{\nu_\mu} CC/\mathrm{POT}$ depends exclusively on the experimental setup. The values of $\langle E_{\nu_\tau} \times \xi_{\nu_\tau} \times r \rangle$, Acc_{ν_τ}, and $\sigma(pA \to D_s^+)/\sigma_{\rm in}(pA)$ are obtained using the QGSM and imposing the conditions of geometrical acceptance for the each experiment.

Finally the $B(D_s^+ \to \tau^+ \nu_\tau)$ is obtained from the most precise recent measurements [24–27] which we show in Fig. 6. For this calculation we have used the weighted mean of the above measurements, $B(D_s \to \tau \nu_\tau) = 4.3 \pm 1\%$. This result is in excellent agreement with the recent value of f_{D_s} obtained from quenched lattice calculations [28], $f_{D_s} = 230 \pm 37$ MeV which yields $B(D_s \to \tau \nu_\tau)$ to be $4.2 \pm 1.3\%$.

V. PROMPT ν_τ BACKGROUND IN CHORUS

In this section we compute the prompt ν_τ background in the CHORUS experiment. We use the same normalization of

TABLE I. $N_{\nu_\tau}CC/N_{\nu_\mu}CC$ for 450 GeV protons on Be and Fe for the CHORUS experiment.

α_ψ	$\frac{\sigma(pA\to D_s^-)}{\sigma_{\rm in}(pA)}$	$\langle E_{\nu_\tau 1}\rangle$	$\mathrm{Acc}_{\nu_\tau 1}$	$\langle E_{\nu_\tau 2}\rangle$	$\mathrm{Acc}_{\nu_\tau 2}$	$\frac{N_{\nu_\tau}CC1}{N_{\nu_\mu}CC}$	$\frac{N_{\nu_\tau}CC2}{N_{\nu_\mu}CC}$
		pBe					
0	$1.\times10^{-4}$	20	8.2×10^{-4}	52	1.8×10^{-3}	2.6×10^{-7}	2.1×10^{-6}
-2.2	1.7×10^{-4}	17	6.7×10^{-4}	45	1.4×10^{-3}	2.7×10^{-7}	2.3×10^{-6}
		pFe					
0	1.7×10^{-4}	21	3.2×10^{-3}	51	6.8×10^{-3}	1.2×10^{-7}	$1.\times10^{-6}$
-2.2	3×10^{-4}	17	2.5×10^{-3}	44	5.5×10^{-3}	1.2×10^{-7}	1.1×10^{-6}

[5], which allows direct comparison with the calculation presented there.

The SPS neutrinos are produced when the 450 GeV protons from the SPS collide against a Be target, 2.7 interaction lengths thick. Following [5], we consider that 93.3% of the protons interact inelastically in the Be target, and the remaining 6.7%, in an iron beam dump located 414 m downstream of the Be target.

The distance between the Be target (Iron beam dump) and the CHORUS experiment is 822 (408) m. The area of the CHORUS target is roughly $1.4\times1.4\ \mathrm{m}^2$, which gives an approximate angular size of 10^{-3} rad for the neutrinos produced in the Be target, and 2×10^{-3} rad for those coming from the iron beam dump. We use the values quoted in [5] for the product $N_A\times\rho\times L=2.7\times10^{-11}$ nucleons/pb and the estimated number of $N_{\nu_\mu}CC/\mathrm{POT}=2.1\times10^{-14}$.

The results for Be, for the two extreme variants of the parameter α_ψ are shown in Table I. The model predicts a total inelastic cross section $\sigma_{\rm in}(p\mathrm{Be})=200$ mb and $\sigma_{pp}^{\rm in}=33.8$ mb. For the charm cross section, we scale the predictions of the model for pp collisions with the atomic weight A according to the results in [29]. We get $\sigma_D=24$ μb/nucleon for the model variant with $\alpha_\psi=0$, and $\sigma_D=43$ μb/nucleon for the model variant with $\alpha_\psi=-2.2$. For both models the fraction of D_s at this energy is predicted to be $\sigma(D_s)/[\sigma(D^0/\overline{D^0})+\sigma(D^\pm)]=0.22$.

However, the variant of the model which predicts larger cross section also predicts a softer x distribution for the charmed hadrons, as shown in Fig. 7. We find that the region of x_{FD_s} which dominates the background production is $\langle x_F\rangle=0.2-0.3$ depending on the model and on the angular acceptance. As a consequence, when convoluted with the small angular acceptance, the two extreme values of the model yield very consistent predictions. Figure 8 shows the energy distribution of the neutrinos reaching the target. As expected, we find than the contribution to the background from $\nu_{\tau 1}$ are 1 order of magnitude smaller than the contribution of $\nu_{\tau 2}$. Given the good agreement of the QGSM predictions with available data and the little dependence on the model parameters, we estimate that the dominant source of uncertainty in our calculation to be the value of the branching ratio for the purely tauonic decay of the D_s and the absolute flux normalization (see next section).

The results for Fe, for the two extreme variants of the parameter α_ψ, are also shown in Table I. The model predicts a total inelastic cross section $\sigma_{\rm in}(p\mathrm{Fe})=700$ mb. Here, again for the charm cross section, we scale the predictions of the model for pp collisions with the atomic weight A. This results in large charm multiplicities for a heavy nucleus such as iron. This, together with the larger angular acceptance, makes the contribution to the background from pFe as large as 50% of the contribution due to pBe collisions.

To summarize: We find a contamination of prompt ν_τ in the CERN-SPS neutrino beam in the CHORUS experiment of the order of

$$\frac{N_{\nu_\tau}CC}{N_{\nu_\mu}CC}\sim3.5\times10^{-6}. \tag{27}$$

This result is consistent with the one obtained by CHORUS [5], $N_{\nu_\tau}CC/N_{\nu_\mu}CC\sim3.3\times10^{-6}$.

VI. PROMPT ν_τ BACKGROUND IN NOMAD

We now pass to evaluate the contamination of prompt ν_τ in the NOMAD experiment. The distance between the Be target (iron beam dump) and the NOMAD experiment is 835 (415) m. The area of the target is roughly $2.6\times2.6\ \mathrm{m}^2$ while its length is $L=4.05$ m. The density of the target is $\rho=91$

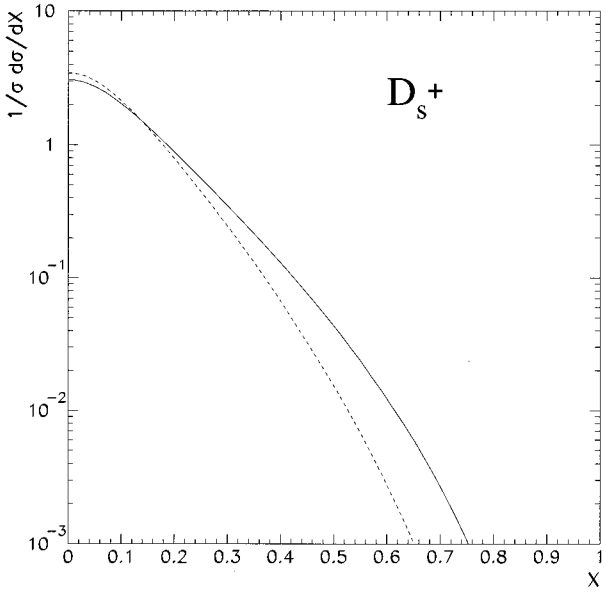

FIG. 7. Predictions of the QGSM for the Feynman-x distributions of D_s mesons in pBe collisions at $E_{\rm lab}=450$ GeV for $\alpha_\psi=0$ (solid line) and $\alpha_\psi=-2.2$ (dashed line).

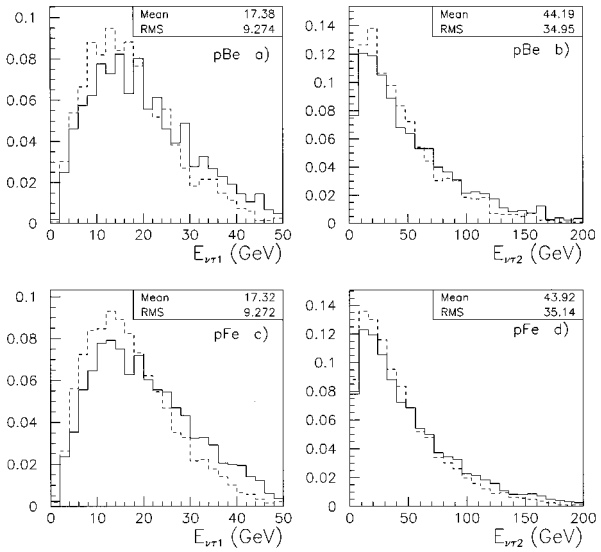

FIG. 8. Predictions of the QGSM for the energy distributions of ν_τ's produced in D_s decay for $\alpha_\psi=0$ (solid line) and $\alpha_\psi=-2.2$ (dashed line) at $E_{\rm lab}=450$ GeV after imposing the angular acceptance cuts. (a) Energy distribution for $\nu_{\tau 1}$ in pBe collision with $\theta_\nu \leqslant 1$ mrad. (b) Same as (a) for $\nu_{\tau 2}$. (c) and (d), same as (a) and (b) for pFe and $\theta_\nu \leqslant 2$ mrad.

kg/m^3 which leads to the product $N_A\times\rho\times L=2.2\times10^{-11}$ nucleons/pb. For incident protons of $p_{\rm lab}=450$ GeV the NOMAD simulation of the beam [30] yields an estimate $N_{\nu_\mu}CC/\mathrm{POT}=4.5\times10^{-14}$.

On the other hand, direct scaling of the CHORUS estimate of $N_{\nu_\mu}CC$/POT (see previous section) by taking into account the beam profile and energy distribution yields a lower number of $N_{\nu_\mu}CC/\mathrm{POT}=4.1\times10^{-14}$. We estimate an error of about 10% in the overall normalization, from the difference in the prediction of the number of $N_{\nu_\mu}CC$/POT due to the difference between the CHORUS description of the SPS beam which scales directly the data from the CHARM II experiment and NOMAD Monte Carlo Program (NUBEAM).

For the angular acceptance we impose the conditions

$$|d\tan(\theta)\sin(\phi)| \leqslant 1.3 \text{ m}$$

and

$$|d\tan(\theta)\cos(\phi)| \leqslant 1.3 \text{ m}, \qquad (28)$$

where d is the distance from the neutrino source to the target and θ and ϕ are the angles determining the ν_τ direction. For the sake of comparison with the CHORUS estimate we quote the approximate angular size which is 2×10^{-3} rad for the neutrinos produced in the Be target, and 4×10^{-3} rad for those coming from the iron beam dump.

As we have seen in the previous section, both variants of the model yield very consistent results. In what follows we will use only variant $\alpha_\psi=-2.2$, which seems to describe better recent experimental data. Our results are summarized in Table II.

TABLE II. $N_{\nu_\tau}CC/N_{\nu_\mu}CC$ for 450 GeV protons on Be and Fe in the NOMAD detector assuming $N_{\nu_\mu}CC/\mathrm{POT}=4.5\times10^{-14}$.

	$\langle E_{\nu_\tau}\rangle$	Acc_{ν_τ}	$\frac{N_{\nu_\tau}CC}{N_{\nu_\mu}CC}$
	pBe		
$\nu_{\tau 1}$	17	2.1×10^{-3}	3.1×10^{-7}
$\nu_{\tau 2}$	44	4.2×10^{-3}	2.7×10^{-6}
	pFe		
$\nu_{\tau 1}$	17	7.6×10^{-3}	1.3×10^{-7}
$\nu_{\tau 2}$	43	1.6×10^{-2}	1.2×10^{-6}

Using the same linear scale for the charm cross section, i.e., the charm multiplicities given in Table I, we find a contamination of prompt ν_τ in the NOMAD experiment

$$\frac{N_{\nu_\tau}CC}{N_{\nu_\mu}CC}\sim 4.5-4.9\times10^{-6} \qquad (29)$$

for $N_{\nu_\mu}CC/\mathrm{POT}=4.5\text{–}4.1\times10^{-14}$.

Thus, one predicts (using the CHORUS normalization) a prompt background for NOMAD of $N_{\nu_\tau}CC/N_{\nu_\mu}CC \sim 5\times10^{-6}$, around 40% higher than for CHORUS. This is due to the larger fiducial area of the NOMAD target. Since prompt ν_τ's are more homogeneously distributed in the beam as compared to the ν_μ's (which are distributed roughly as a Gaussian of 1 m standard deviation in the NOMAD target), the prompt background increases with the transverse size of the detector.

VII. FUTURE τ NEUTRINO EXPERIMENTS

Clearly, the estimated level of prompt ν_τ contamination is not a serious problem for the CHORUS and NOMAD ex-

TABLE III. $N_{\nu_\tau}CC/N_{\nu_\mu}CC$ for a future experiment running at the SPS beam at 350 GeV and 120 GeV.

$E_{\rm lab}$	$\frac{\sigma(pA\to D_s^-)}{\sigma_{\rm in}(pA)}$	$\langle E_{\nu_\tau 1}\rangle$	$\mathrm{Acc}_{\nu_\tau 1}$	$\langle E_{\nu_\tau 2}\rangle$	$\mathrm{Acc}_{\nu_\tau 2}$	$\frac{N_{\nu_\tau}CC1}{N_{\nu_\mu}CC}$	$\frac{N_{\nu_\tau}CC2}{N_{\nu_\mu}CC}$
		pBe					
350	1.1×10^{-4}	13.	3.7×10^{-4}	36.	7.4×10^{-4}	7.4×10^{-8}	8.1×10^{-7}
120	1.8×10^{-5}	5.3	8.6×10^{-5}	18.	1.1×10^{-4}	2.8×10^{-9}	6.1×10^{-8}
		pFe					
350	1.9×10^{-4}	13	1.5×10^{-3}	35.	2.9×10^{-3}	3.8×10^{-8}	3.8×10^{-7}
120	3.2×10^{-5}	5.2	3.3×10^{-4}	18	4.5×10^{-4}	1.4×10^{-9}	3.1×10^{-8}

TABLE IV. Expected number of background events from prompt ν_τ's at the Cosmos experiment.

	$\langle E_{\nu_\tau}\rangle$	Acc_{ν_τ}	$\frac{\sigma(pA\to D_s^-)}{\sigma_{\mathrm{in}}(pA)}$	$N_{\nu_\tau}CC$
		pC		
$\nu_{\tau 1}$	5.2	3.3×10^{-4}	2.1×10^{-5}	0.011
$\nu_{\tau 2}$	18	4.5×10^{-4}	2.1×10^{-5}	0.25
		pFe		
$\nu_{\tau 1}$	5.2	3.5×10^{-3}	3.2×10^{-5}	0.047
$\nu_{\tau 2}$	17	4.3×10^{-3}	3.2×10^{-5}	0.86

periments. In both experiments one expects less than one event due to prompt ν_τ background. However, a future $\nu_\mu(\nu_e)\leftrightarrow\nu_\tau$ oscillation experiment aiming at improving the sensitivity of both CHORUS and NOMAD by an order of magnitude has to find a way to reduce this contamination.

The most straightforward solution to reduce the prompt ν_τ background is to lower the SPS beam energy. This is, in addition, interesting from the point of view of the search motivation. If CHORUS and NOMAD find a negative result, the main interest of a future $\nu_\mu(\nu_e)\leftrightarrow\nu_\tau$ oscillation experiment will be to explore the region of low mass difference rather than pushing the asymptotic sensitivity to the mixing angle [31]. To that extent, reducing the SPS beam energy favors exploring the lower mass region.

A drastic reduction of the SPS beam energy (i.e., by about 1/3 thus going to beam energies of 120–150 GeV), although the best option from the point of view of exploring the low mass region, would require solving a number of challenging problems in order to compensate for the reduced ν_μ flux. On the other hand, it has been shown [32] that operating the SPS at 350 GeV presents little complication and almost no loss of ν_μ flux. One is then interested in evaluating the prompt ν_τ background at this energy.

Thus, we have computed the expected prompt ν_τ contamination for a 350 GeV and a 120 GeV beam, to evaluate the relevance of this background for ''conservative'' (350 GeV) and ''aggressive'' (120 GeV) modifications of the SPS beam energy. We have assumed a detector along the lines in the NAUSICAA and TENOR proposals [33–35], i.e., a compact, and dense emulsion target. For this calculation we consider a target of about 4 tons, with the same transverse dimensions of CHORUS but five times more massive. We use the NOMAD simulation of the beam to estimate a number of $N_{\nu_\mu}CC/\mathrm{POT}=8.0(0.87)\times10^{-14}$ for protons of 350 (120) GeV.

Our results are summarized in Table III. We find a contamination of prompt ν_τ,

$$\frac{N_{\nu_\tau}CC}{N_{\nu_\mu}CC}\sim 1.3\times10^{-6}--9.6\times10^{-8} \tag{30}$$

at 350–120 GeV.

A future experiment at the CERN-SPS, running for a total of 3 years, with a target mass of 4 tons, can collect roughly 5×10^6 $\nu_\mu CC$. As discussed in [34,35] this experiment would yield a high τ detection efficiency, typically 30–50 %. Thus, at a low beam energy of 120 GeV, the prompt ν_τ background is totally negligible, while about a total of 2–3 prompt ν_τ's would be detected at 350 GeV. Furthermore, those neutrinos have an average energy far in excess of the energy of the τ neutrinos arising from a potential $\nu_\mu(\nu_e)\leftrightarrow\nu_\tau$ oscillation, particularly for low values of Δm^2. One can then conclude that even at 350 GeV, the prompt background would not be a serious problem for a future $\nu_\mu(\nu_e)\leftrightarrow\nu_\tau$ experiment at the CERN-SPS neutrino beam.

TABLE V. Expected number of ν_τ charged current at the P872 proposed experiment.

	$\langle E_{\nu_\tau}\rangle$	Acc_{ν_τ}	$\frac{\sigma(pW\to D_s^-)}{\sigma_{\mathrm{in}}(pW)}$	$N_{\nu_\tau}CC$
$\nu_{\tau 1}$	21	0.093	$8.\times10^{-4}$	19
$\nu_{\tau 2}$	54	0.14	$8.\times10^{-4}$	122

We have also studied the expected background from prompt ν_τ's at the COSMOS experiment [6] which has been approved to run at Fermilab using the main injector which will deliver a total of 13×10^{20} 120-GeV protons on a Graphite target at 470 m of the detector where 80% of the primary beam interacts. The remaining protons are stopped in an iron beam dump only 150 m from the detector. The proposed detector is a hybrid emulsion-electronic spectrometer. The emulsion target is comprised of two stalks, each 1.8 m wide, 1.4 m high, and 3 cm thick which amounts for a total emulsion mass of 0.52 ton. With this we obtain

$$N_{CC\nu_\tau i}=1.1\times10^8\times\langle E_{\nu_\tau i}\times r\times\xi_i\rangle\times\frac{\sigma(pA\to D_s^-)}{\sigma_{\mathrm{in}}(pA)}\times B(D_s^+\to\tau^+\nu_\tau). \tag{31}$$

We display our results in Table IV. Again to scale the multiplicities from pp to pA we have used the total inelastic cross sections $\sigma_{\mathrm{in}}(p\mathrm{C})=230$ mb, $\sigma_{\mathrm{in}}(p\mathrm{Fe})=700$ mb, and $\sigma_{pp}^{\mathrm{in}}=31$ mb at $E_{\mathrm{lab}}=120$ GeV. As seen in the table, we find that the main source of background is charm production in the iron beam dump. Taking into account the expected detection efficiency for ν_τ's of about 15% we find that the number of background events from prompt neutrinos is 0.17 detected events which agrees well with the prediction quoted in the proposal.

Finally we have estimated the expected rate of ν_τ interactions for the proposed experiment E872 [2] at Fermilab using the QGSM. This experiment attempts to detect directly the τ leptons produced in the charged current interaction of the τ neutrinos using the Fermilab 800 GeV proton beam. The experiment expects an integrated luminosity of 2×10^{18} protons colliding on a Tungsten beam dump. The detector is an emulsion target with a density $\rho=3.72$ g/cm^3 located at a distance of 35 m from the dump. The area of the emulsion will be approximately 60×60 cm^2, and the target is arranged in six 2.5 cm thick modules. We can then write

$$N_{CC\nu_\tau i}=N_{\mathrm{prot}}\times\frac{\sigma(pW\to D_s^-)}{\sigma_{\mathrm{in}}(pW)}\times B(D_s^+\to\tau^+\nu_\tau)\times\mathrm{Acc}_{\nu_\tau i}\times(\sigma_{\nu i}+\sigma_{\bar{\nu}i})\times N_A\times\rho\times L \tag{32}$$

since the experiment is interested in detecting both neutrinos and antineutrinos. This leads to

$$N_{CC\nu_\tau i} = 6.8\times 10^5 \times \mathrm{Acc}_{\nu_\tau i} \times \langle E_{\nu_\tau i} \times r \times \xi_i \rangle \times \frac{\sigma(pW \to D_s^-)}{\sigma_{\mathrm{in}}(pW)} \times B(D_s^+ \to \tau^+ \nu_\tau). \quad (33)$$

Our results are shown in Table V where we have used that $\sigma_{\mathrm{in}}(pW) = 1650$ mb and $\sigma_{pp}^{\mathrm{in}} = 34$ mb at $E_{\mathrm{lab}} = 800$ GeV. We obtain a total yield of 141 ν_τ charged current interactions which is 35 % lower than the 222 predicted in the proposal.

VIII. CONCLUSIONS

We have used the QGSM as theoretical framework to compute a consistent set of predictions of ν_τ fluxes due to the tauonic decay of the D_s, in different experiments. Specifically we compute the expected ν_τ prompt background due to D_s decays in the SPS neutrino beam for both the NOMAD and CHORUS experiments, the expected ν_τ prompt background for the COSMOS experiment and the expected number of interactions for the E872 experiment. Finally we compute the expected ν_τ prompt background for a future $\nu_\mu(\nu_e) \leftrightarrow \nu_\tau$ oscillation experiment at CERN-SPS. We find that with a moderate decrease in the SPS beam energy (operating at 350 GeV) this background can be reduced to a manageable level and it becomes negligible at a low energy (i.e., 120 GeV).

[1] A. De Rujula, E. Fernandez, and J. Gomez-Cadenas, Nucl. Phys. **B405**, 80 (1993).

[2] B. Lundberg *et al.*, Fermilab Report No. P872, 1994 (unpublished).

[3] CHORUS Collaboration, N. Armenise *et al.*, Report No. CERN-SPSC/90-42, 1990 (unpublished).

[4] NOMAD Collaboration, P. Astier *et al.*, CERN Report No. CERN-SPSLC/91-21, 1991 (unpublished); CERN-SPSLC/91-48 1991 (unpublished); Report No. SPSLC/P261 Add. 1, 1991 (unpublished).

[5] B. Van de Vyver and P. Zucchelli, CERN Report No. CERN-PPE/96-113 (unpublished).

[6] K. Kodama *et al.*, Fermilab Report No. P803, 1993 (unpublished).

[7] G. 't Hooft, Nucl. Phys. **B72**, 461 (1974).

[8] G. Veneziano, Nucl. Phys. **B74**, 365 (1974); **B117**, 519 (1976).

[9] A. B. Kaidalov, Phys. Lett. **116B**, 459 (1982); A. B. Kaidalov and K. A. Ter-Martirosyan, *ibid.* **117B**, 247 (1982); Sov. J. Nucl. Phys. **39**, 979 (1984).

[10] A. B. Kaidalov, Sov. J. Nucl. Phys. **45**, 902 (1987); **33**, 733 (1981).

[11] Y. M. Shabelski, Sov. J. Nucl. Phys. **44**, 117 (1986); A. B. Kaidalov and O. I. Piskunova, *ibid.* **41**, 816 (1985).

[12] A. B. Kaidalov and O. I. Piskunova, Sov. J. Nucl. Phys. **43**, 994 (1986).

[13] G. I. Lykasov and M. N. Sergeenko, Sov. J. Nucl. Phys. **55**, 1393 (1992).

[14] Y. M. Shabelski, Sov. J. Part. Nucl. **12**, 430 (1981); A. B. Kaidalov, K. A. Ter-Martirosyan, and Y. M. Shabelski, Sov. J. Nucl. Phys. **43**, 822 (1986); Y. M. Shabelski, Z. Phys. C **38**, 569 (1988).

[15] V. Blobel *et al.*, Nucl. Phys. **B69**, 454 (1974).

[16] A. B. Kaidalov and O. I. Piskunova, Z. Phys. C **30**, 145 (1986).

[17] See, for example, A. Capella *et al.*, Phys. Rep. **236**, 225 (1994), and references therein.

[18] M. Aguilar-Benitez *et al.*, Phys. Lett. B **189**, 476 (1987); **201**, 176 (1988); Z. Phys. C **40**, 321 (1988); R. Ammar *et al.*, Phys. Lett. B **182**, 110 (1986).

[19] O. Botner *et al.*, Phys. Lett. B **236**, 488 (1990).

[20] E769 Collaboration, G. A. Alves *et al.*, Phys. Rev. Lett. **77**, 2392 (1996).

[21] HELIOS Collaboration, T. Akesson *et al.*, CERN Report No. CERN-PPE/96-23, 1996 (unpublished).

[22] H. Koppe, Phys. Rev. **76**, 688 (1949); E. Fermi, Prog. Theor. Phys. **5**, 570 (1950).

[23] R. Hagedorn, CERN Report No. 71-12 (unpublished), and references therein.

[24] CLEO Collaboration, D. Acosta *et al.* Phys. Rev. D **49**, 5690 (1994); Report No. CLEO CONF 95-22 EPS0184, 1995 (unpublished).

[25] WA75 Collaboration, S. Aoki, *et al.*, Prog. Theor. Phys. **89**, 131 (1993).

[26] E653 Collaboration, K. Kodama *et al.*, Phys. Lett. B **382**, 299 (1996).

[27] L3 Collaboration (unpublished).

[28] C. W. Bernard, J. N. Labrenz, and A. Soni, Phys. Rev. D **49**, 2536 (1994).

[29] E789 Collaboration, M. J. Leitch *et al.*, Phys. Rev. Lett. **72**, 2542 (1994).

[30] S. Tovey *et al.*, NOMAD Report No. 95-030, 1995 (unpublished).

[31] See, for example, J. J. Gomez-Cadenas and M. C. Gonzalez-Garcia, Z. Phys. C **71**, 443 (1996), and references therein.

[32] E. Tsesmelis (private communication).

[33] J. J. Gomez-Cadenas, J. A. Hernando, and A. Bueno, Nucl. Instrum. Methods Phys. Res. A **A378**, 196 (1996).

[34] J. J. Gomez-Cadenas and J. A. Hernando, CERN Report No. CERN-PPE/96-69 (unpublished).

[35] A. Ereditato, G. Romano, and P. Strolin, CHORUS Report No. 96-03 (unpublished).